

# The double quasar Q2138-431: detection of a lensing galaxy

M. R. S. Hawkins<sup>1</sup>★

<sup>1</sup>*Institute for Astronomy (IfA), University of Edinburgh, Royal Observatory, Blackford Hill, Edinburgh EH9 3HJ, UK*

Accepted XXX. Received YYY; in original form ZZZ

## ABSTRACT

This paper reviews the question of whether the wide separation double quasar Q2138-431 is a gravitational lens. From early work, the two quasar images are known to have almost identical spectra and redshifts, but no lensing galaxy has so far been detected. In this paper we used recent deep surveys in infrared and optical bands to search for the presence of a galaxy with the expected properties of a gravitational lens. The search revealed a  $5\sigma$  detection of a faint galaxy between the two quasar images on a deep  $J$ -band frame from the VISTA Science Archive, with apparent magnitude  $J = 20.68$ . Non-detection in the  $I$ -band implied a redshift  $z > 0.6$ , and mass modelling of the quasar system gave a mass of  $1.31 \times 10^{12} M_{\odot}$  for the lensing galaxy, with mass-to-light ratio  $M_{\odot}/L_{\odot} = 9.0$ . Archival photographic data from the UK 1.2m Schmidt telescope covering 25 years were used to construct light curves for the two quasar images, which were then cross-correlated to measure any time lag. This showed image B to lead image A by around a year, consistent with 410 days from the mass model. Although the similarity of the spectra and the detection of the lensing galaxy are the most compelling arguments for the classification of Q2138-431 as a gravitational lens, the time delay and mass-to-light ratio provide a consistent picture to support this conclusion. The wide separation of the quasar images and the simplicity of the mass model make Q2138-431 an excellent system for the measurement of the Hubble constant.

**Key words:** quasars: individual (Q2138-431) – gravitational lensing: strong

## 1 INTRODUCTION

The double quasar Q2138-431 was discovered as part of a photographic survey for quasars based on optical variability (Hawkins et al. 1997). It was detected as an elongated blue image which varied by over a magnitude in a few years, and closer inspection showed it to comprise two star-like images separated by about 4.5 arcsec. Subsequent analysis, which we briefly review in Section 2, revealed that the two images were quasars with the same redshift,  $z = 1.641$ . This raised the possibility that the quasar images were part of a gravitational lens system, although there was no obvious sign of a lensing galaxy. In Fig. 1 we have constructed a composite 3-colour image using frames from the Dark Energy Survey (DES) (Abbott et al. 2018) in the  $g$ ,  $r$  and  $i$  passbands. The two quasar images are clearly visible near the centre, together with a sparse population of mostly red galaxies with a limiting magnitude of  $R \approx 24$ .

Wide separation gravitational lenses with image separations greater than two arcsecs are rare, and have proved particularly useful in investigating dark matter distributions (Fadely et al. 2010), and the measurement of the Hubble constant (Eigenbrod et al. 2005; Suyu et al. 2013; Wong et al. 2017). Should Q2138-431 be shown to be a two-component gravitational lens, it would be among the widest separation systems known, and very well suited to mass modelling and the measurement of a time delay for calculating the Hubble constant. In the CASTLES<sup>1</sup> database of gravitational lenses, there are only

five systems with separations greater than 4 arcsec. Two of these are quadruple cluster lenses (Oguri et al. 2008; Fohlmeister et al. 2008; Hawkins 2020), which although interesting in their own right present major difficulties for the measurement of the Hubble constant. The remaining three are doubles, of which RXJ 0921+4529 has now been shown to be a binary system (Popović et al. 2010). CLASS B2108+213, which was discovered as a double lensed radio source with a smooth optical spectrum, is tentatively identified as a BL Lac object (McKean et al. 2005, 2010). So far the source redshift has not been measured, and the complexity of the lensing group or cluster suggests some difficulty in measuring the value of the Hubble constant. The final large separation lens is the well-known double Q0957+561 (Walsh et al. 1979) which has indeed proved useful for the measurement of the Hubble constant (Fadely et al. 2010), but even here the asymmetry of the positions of the quasar images and galaxy lenses has complicated the modelling of the system.

In the paper reporting the discovery of the double quasar Q2138-431, Hawkins et al. (1997) showed that the spectra of the two quasar images are almost identical, and that the redshifts are the same to within very small errors. This made a strong case for the two images to be gravitationally lensed, but long CCD integrations in the  $R$ -band failed to reveal a lensing galaxy. For this paper we have taken advantage of modern deep photometric surveys, especially in the infrared, to look again for a lensing galaxy between the two quasar images. Image subtraction of the quasar images has resulted in the positive  $5\sigma$  detection of a galaxy in the  $J$ -band, but no significant detections in the  $r$ -,  $i$ - or  $z$ -bands. We used the photometry in these passbands to estimate a lower limit to the redshift of the lensing

★ E-mail: mrsh@roe.ac.uk

<sup>1</sup> <https://www.cfa.harvard.edu/castles/>



**Figure 1.** Composite 3-colour image from DES frames in  $g$ ,  $r$  and  $i$  passbands, showing the galaxy environment of the two quasar images near the centre of the frame, with the brighter image A to the right and image B to the left. The field also includes some of the local standard stars used for the measurement of the light curve. The frame is approximately 20 arcsec on a side, and north is up the page, east to the left.

galaxy, and hence its absolute magnitude. We also used astrometric measurements of the positions of the quasar images and lensing galaxy to fit a mass model to the system, and obtain a value for the mass of the deflector. The resulting parameters imply that the lens is a massive luminous red galaxy (LRG). The survey data on which this analysis is based is described in Section 2, and the image analysis techniques and photometry in Section 3.

For a gravitational lens system to be useful for the measurement of the Hubble constant, it is necessary to measure time delays between the light paths to the images. The photographic survey which resulted in the discovery of Q2138-431 is described in more detail in Section 2, and comprised long runs of yearly observations in several passbands between the years 1977 and 2001. These plates yield light curves for the two quasar images which can be cross-correlated to provide a preliminary estimate of the time lag between variations in the two images, which we describe in Section 4. We then compare this result with the predicted time delay from the mass model. Throughout the paper we assume  $\Omega_M = 0.27$ ,  $\Omega_\Lambda = 0.73$  and  $H_0 = 71 \text{ km s}^{-1} \text{ Mpc}^{-1}$  for cosmological calculations.

## 2 OBSERVATIONS

The double quasar Q2138-431 was discovered as part of a survey for variable objects with an ultra-violet excess and an elongated image on photographic plates from the 1.2m UK Schmidt telescope at Siding Springs Observatory, Australia (Hawkins et al. 1997). The purpose of the survey was to find gravitationally lensed quasars, and Q2138-431 was the most promising candidate which on closer examination was seen to comprise two images separated by 4.5 arcsec. Spectroscopy of the two images was obtained with the ESO 3.6m telescope at La Silla, Chile, which showed them to be quasars with no detectable difference between the two high signal-to-noise spectra, as illustrated

in Figure 2 of Hawkins et al. (1997). The redshifts of the two quasar images were the same at  $z = 1.641$ , and cross-correlation between the two spectra showed a difference in velocity of  $0 \pm 114 \text{ km s}^{-1}$ . Such a small velocity difference is hard to account for in a random alignment or binary pair, and strongly suggested that the quasar images were part of a gravitational lens system. There was however no obvious evidence for a lensing galaxy. In order to clarify the situation, deep CCD observations of the quasar images were obtained in the  $R$ -band, and the area between the two quasar images investigated using image subtraction techniques to reduce contamination from the quasar light. No lensing galaxy was detected, with a lower limit of  $R > 23.8$ .

The failure to find a lensing galaxy suggested the possibility that the lens might be a dark galaxy, an idea which was receiving some attention at that time (Hawkins 1997). However, the limit obtained in the  $R$ -band is only useful for relatively low redshift lenses. The 4000 Å feature starts to leave the  $R$ -band at around  $z \approx 0.4$  and from the  $I$ -band at  $z \approx 0.8$ , making the detection of a lensing galaxy in this regime very challenging. On this basis we moved the search into the infrared, and made use of the  $J$ -band survey from the VISTA Science Archive<sup>2</sup> (VSA). The archive contains image tiles which we used for the detection of the lensing galaxy, and catalogue data which we used for calibration. The details of the analysis are described in Section 3. In addition to the  $J$ -band data, we also made use of  $r$ -,  $i$ - and  $z$ -band data from the Dark Energy Survey<sup>3</sup> (DES) (Abbott et al. 2018) to look for detections or upper limits in the reddest available optical bands. Data from this survey were also used for the construction of a local sequence to calibrate the light curves described in Section 4. The light curves themselves were measured from an extension of the series of photographic plates used in the discovery of Q2138-431, and the SuperCOSMOS scans form part of the SuperCOSMOS Science Archive<sup>4</sup> (SSA). The measurement and analysis of the light curves of the two quasar images is described in detail in Section 4.

## 3 THE LENSING GALAXY

### 3.1 Infrared observations

The Q2138-431 system has celestial coordinates  $21^{\text{h}} 41^{\text{m}} 16.27^{\text{s}}$ ,  $-42^\circ 57' 10.0''$  (2000) and in the VISTA Science Archive is covered by frames in the  $J$  and  $K_s$  passbands. The frames have a pixel size of 0.341 arcsec, and median seeing FWHM = 1.18 arcsec. In Fig. 2 we show cutouts from these frames, with the double quasar at the top, and below it a star which has been helpful in the photometric calibration and for image subtraction. cursory examination of the  $J$ -band image in the left hand panel shows a suggestive bulge along the line of centres of the two quasar images, which has the potential to be the lensing galaxy. The  $K_s$ -band image in the right hand panel of Fig. 2 does not show this feature, but the frame does not go very deep, and indeed image B of the double quasar is barely visible. We discuss detection limits in detail below.

In order to investigate the possibility that the feature between the quasar images is the lensing galaxy, we undertook a PSF subtraction procedure to remove the contaminating quasar light. Attempts to use stars in the field as models for the PSF, including the one visible in Fig. 2, were not very successful due to difficulties in registration and

<sup>2</sup> <http://horus.roe.ac.uk/vsa/>

<sup>3</sup> <https://des.ncsa.illinois.edu/releases/dr1>

<sup>4</sup> <http://ssa.roe.ac.uk>

poor signal-to-noise. The best approach proved to be to use a Moffat profile (Trujillo et al. 2001) of the form:

$$P(r) = h \left[ 1 + \left( \frac{r}{\alpha} \right)^2 \right]^{-\beta} \quad (1)$$

fitted to a star of similar magnitude to the quasar images. We first rebinned the array to improve registration giving the images shown in the left hand panel of Fig. 3, and then measured the image centroids with the Starlink GAIA package. The next step was to fit the Moffat profile to the star in Fig. 2. We followed Trujillo et al. (2001) and set  $\beta = 4.765$ , and then varied  $\alpha$  and  $h$  to give the best fit. For the PSF subtraction we kept these values of  $\alpha$  and  $\beta$  and for each of the two quasar images varied  $h$  to get the best fit. The resulting profiles  $P(r)$  were then subtracted from each image using the measured centroids. The results of this procedure are shown in the right hand panel of Fig. 3. Contours of the subtracted quasar images are included to show the location and shape of the galaxy image.

In order to assess the likelihood that we had a detection of the lensing galaxy, the first step was to measure its brightness. To do this, we used local photometric standards from the VSA catalogue, and then with photometry routines from the GAIA package we measured the apparent magnitude of the lensing galaxy to be  $J = 20.68 \pm 0.09$ . Based on the rms variation of the sky background, this is a  $5\sigma$  detection. The detection limit of the frame was determined from the faintest  $5\sigma$  detections listed in the VSA catalogue, and verified by our photometry of the faintest images observed on the frame covering the quasar position. The  $5\sigma$  detection limit we derived was  $J \lesssim 20.7$ .

The right hand panel of Fig. 2 shows the quasar system on the  $K_s$  frame from the VSA survey. Visual inspection of the area between the two quasar images shows no evidence for the presence of a lensing galaxy. The  $K_s$  frame is clearly less deep than the one for the  $J$ -band, and the B image of the quasar is very faint, but we found it useful to measure the detection limit to put bounds on the colour of the lensing galaxy and its redshift. Using the same approach as for the  $J$ -band we found the detection limit to be  $K_s \lesssim 18.7$ . To estimate the  $K_s$  magnitude of the lensing galaxy we used the intrinsic colours for luminous red galaxies (LRGs) from Mannucci et al. (2001). For the  $J - K$  passband they give  $J - K = 0.87$ , which implies  $K_s \gtrsim 19.8$ , well below the detection limit of the  $K_s$  frame and consistent with non-detection in the  $K_s$  passband. Applying  $K$  and evolutionary corrections from Poggianti (1997) up to a redshift  $z \sim 1$  does not significantly alter this.

### 3.2 Optical observations

In addition to the  $J$ - and  $K_s$ -band images from the VSA survey, the Q2138-431 system was also observed as part of the Dark Energy Survey in the  $g$ ,  $r$ ,  $i$  and  $z$  passbands (Abbott et al. 2018). These frames have a pixel size of 0.263 arcsec with a median seeing FWHM = 0.94 arcsec, and proved very useful in putting limits on the redshift of the lensing galaxy. To estimate the expected magnitudes of the lensing galaxy in these passbands, we again made use of the intrinsic colours of Mannucci et al. (2001), based on template spectra of a large sample of galaxies. We converted the Johnson colours of Mannucci et al. (2001) to the SDSS system using the colour transformations of Jordi et al. (2006). These were then applied to the observed  $J$  magnitude of the lensing galaxy to obtain estimated magnitudes of  $g = 23.56$ ,  $r = 22.73$ ,  $i = 22.36$  and  $z = 22.18$  in the galaxy rest frame. Examination of the DES frames showed no indication of the presence of a lensing galaxy, in agreement with the results of Hawkins et al. (1997) from CCD frames of similar depth to the DES observations. The 95%

**Table 1.** Summary of the observations for Q2138-431 used in the lens modelling.

Observations		A	B	G
Positions	RA (arcsec)	$4.117 \pm 0.02$	0	$2.815 \pm 0.02$
	Dec (arcsec)	$1.558 \pm 0.02$	0	$1.259 \pm 0.02$
Fluxes	$J$ (mags)	$18.24 \pm 0.03$	$19.85 \pm 0.07$	$20.68 \pm 0.09$

completeness limits in these passbands (Abbott et al. 2018) are  $g < 23.72$ ,  $r < 23.35$ ,  $i < 22.88$  and  $z < 22.25$ . In all cases the estimated rest wavelength magnitudes are within these bounds, and so the non-detections can be used to set minimum values for the  $K$  corrections, and hence the minimum redshift of the lensing galaxy. As might be expected, the non-detection in the  $i$ -band provides the strongest constraint on the redshift of the lensing galaxy. Using  $K$  corrections from Poggianti (1997), the minimum redshift for the lensing galaxy to move below the detection threshold is  $z \gtrsim 0.5$ .

So far, we have neglected the possible effect of an evolutionary correction in our calculations. Evolutionary corrections can be unreliable and model dependent (D’Souza et al. 2015), but this can be allowed for by comparing the observed lower limit to the  $i - J$  colour with the intrinsic  $(i - J)_0$  colour. In this case, the large evolutionary corrections largely cancel out, and the redshift can be estimated by determining the point at which the addition of the combined  $K + e$  correction to the intrinsic colour matches the observation. We find that  $(i - J)_{obs} > 2.2$ , and  $(i - J)_0 = 1.7$  implying a  $K + e$  correction of 0.5, corresponding to a redshift of  $z > 0.6$ . The inclusion of the evolutionary correction thus slightly tightens the redshift limit.

A lower limit to the redshift of the lensing galaxy of around  $z \gtrsim 0.6$  is not surprising, given the faintness of the  $J$  magnitude, and provides an explanation as to why the lens galaxy is not detected in optical passbands. The lower limit on  $z$  also implies a lower limit on the luminosity of the lensing galaxy. Using the  $K$  and evolutionary corrections for  $z = 0.6$  from Poggianti (1997), we obtain  $M_J = -21.02$ . Applying a bolometric correction  $BC = 2.13$  for the VISTA  $J$ -band frames from Choi et al. (2016) gives an absolute magnitude  $M_{bol} = -23.15$ , equivalent to a luminosity  $L_{gal} = 1.45 \times 10^{11} L_{\odot}$ .

### 3.3 Lens model

To provide a consistent picture of the properties of the lensing galaxy, we made use of the lens modelling software of Keeton (2001) to estimate the lens mass. We used the GAIA astrometry package to measure the positions of the two quasar images, obtaining a refined value for the image separation of 4.481 arcsec, and also the position of the lensing galaxy.  $J$ -band flux measures for the two quasar images from the VISTA frame were also included in the lens model. We then used routines from the software of Keeton (2001) to fit a singular isothermal ellipsoid plus external shear (SIE +  $\gamma$ ) model to the astrometric and photometric data, which are summarised in Table 1. We obtained a good fit to the positions, and derived a value for the Einstein radius of  $\theta_E = 2.019$  arcsec, close to that found by Hawkins et al. (1997). We obtained  $e = 0.1$  for the lens ellipticity, in position angle  $-10^\circ$  measured east of north. For the external shear we found  $\gamma = 0.1$  in position angle  $40^\circ$ . The overall goodness of fit gave  $\chi^2 = 12.6$ .

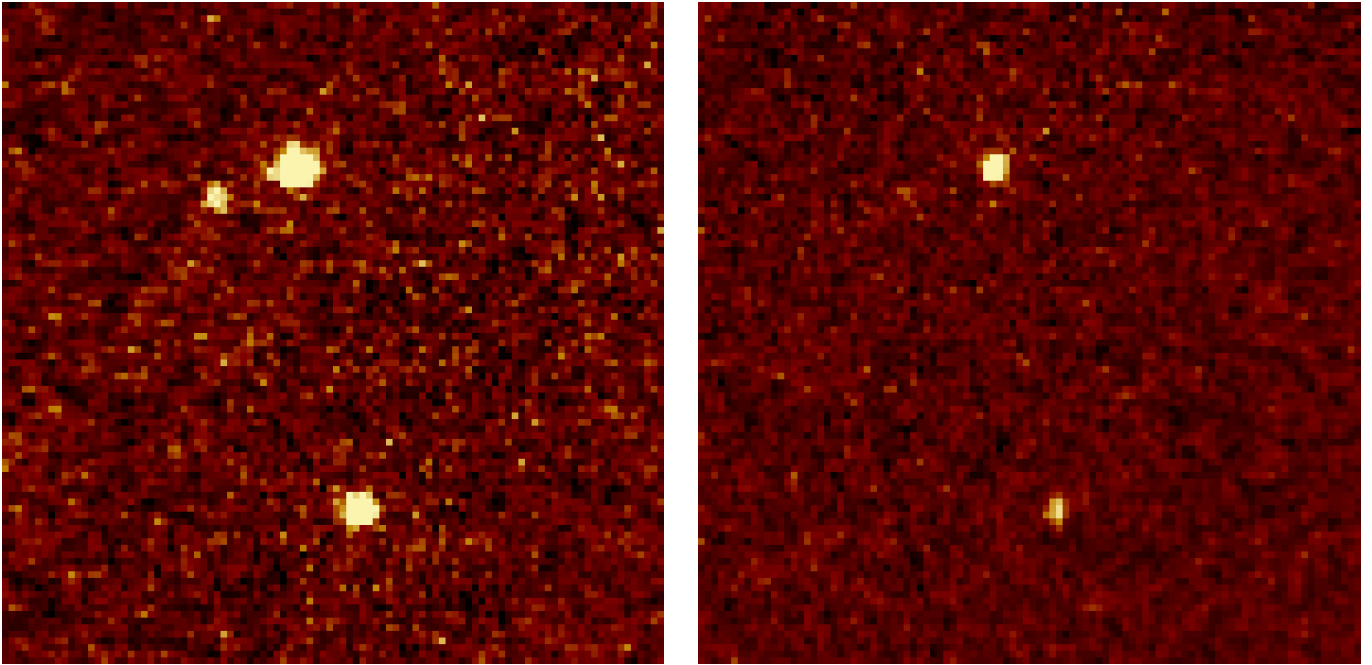


**Figure 2.** Frames from the VISTA Science Archive in the  $J$ -band (left hand panel) and  $K_s$ -band (right hand panel). The frames are approximately 30 arcsec on a side, and north is up the page, east to the left. The frames show the double image of Q2138-431 at the top, with image A to the right and image B to the left, and a nearby star used to fit the PSF below.

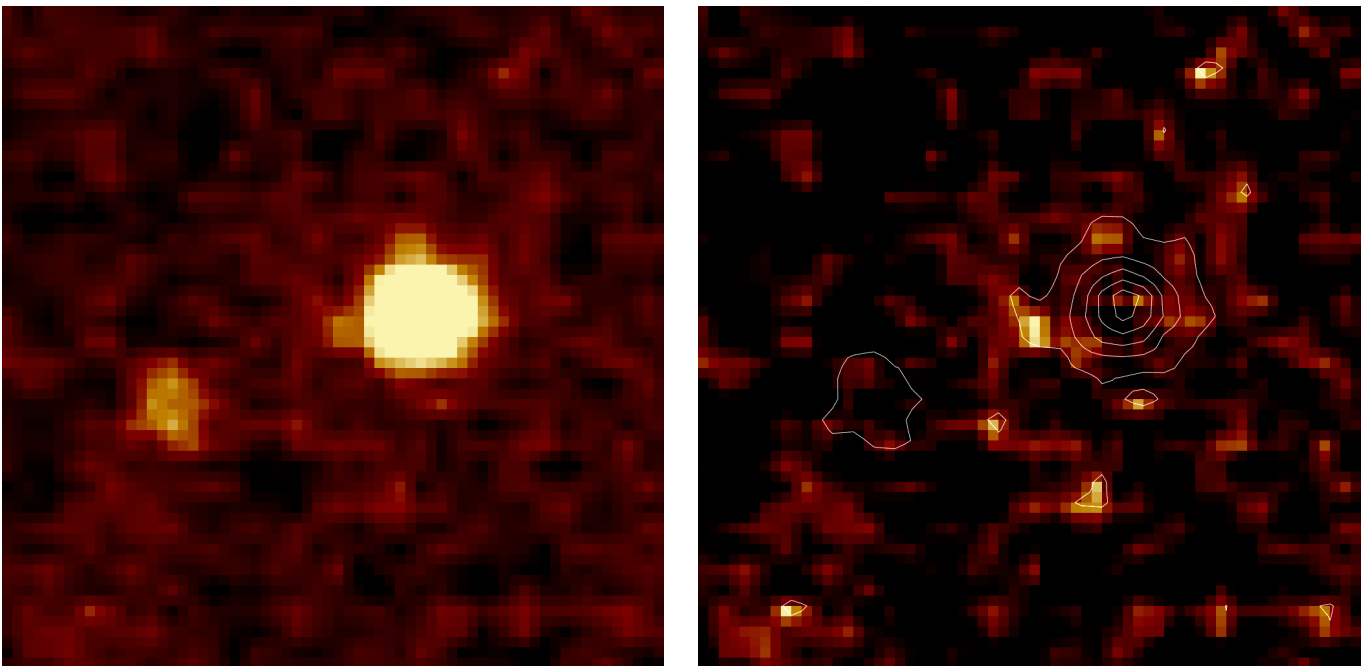


**Figure 3.** The left hand panel is from a  $J$ -band frame from the VISTA Science Archive. The frame has been re-binned and shows image A to the right and image B to the left. The small bulge extending to the left of image A is the candidate lensing galaxy. In the right hand panel the quasar light has been subtracted, clearly revealing the presence of a galaxy between the two quasar images, the positions of which are indicated by superimposed contours. The plots are approximately 10 arcsec on a side, and north is up the page, east to the left.

The mass  $m$  of the lens depends mainly on  $\theta_E$ , but is also a function of the quasar and galaxy redshifts. To be specific,

$$m = \frac{c^2 \theta_E^2}{4G} \frac{D_{LS}}{D_L D_S} \quad (2)$$

where  $D_L$ ,  $D_S$  and  $D_{LS}$  are the angular diameter distances to the lens, to the source, and from the lens to the source respectively. Using the lower limit  $z = 0.6$  derived above, this gives  $m_{lens} = 1.31 \times 10^{12} M_\odot$ . Combining this limit with the luminosity limit  $L_{gal} = 1.45 \times 10^{11} L_\odot$  derived above gives a mass-to-light ratio  $M_\odot/L_\odot = 9.0$ . To give an idea of the sensitivity of this result to redshift, if we assume  $z = 1.0$  then  $m_{lens} = 2.88 \times 10^{12} M_\odot$ ,  $L_{gal} = 3.53 \times 10^{11} L_\odot$  and  $M_\odot/L_\odot = 8.2$ .

#### 4 LIGHT CURVES

The discovery of Q2138-431 was part of a long term survey to detect quasars on the basis of their variability (Hawkins 1996). The survey was based on an extensive sequence of photographic plates in several colours taken with the UK 1.2m Schmidt Telescope of the ESO/SERC field 287, centred on  $21^{\text{h}} 28^{\text{m}}, -45^\circ$  (1950). Of particular interest for the detection of quasars is the  $B_J$  passband, bounded by the GG395 filter in the blue, and the IIIaJ emulsion cut-off in the red at about  $5400 \text{ \AA}$ , and quite close to the SDSS  $g$ -band. The plates were originally measured with the COSMOS measuring machine at the Royal Observatory, Edinburgh (MacGillivray & Stobie 1984), which after photometric calibration produced light curves covering some 16 years. Although these light curves were sufficient to detect a large number of quasars from their variability, including Q2138-431, the machine measures used a low detection threshold above the sky, which merged the two quasar images. This meant that the light curves of the two images could not be measured separately. Since the discovery of Q2138-431, the original sequence of plates in the  $B_J$  passband has been extended to include at least one plate, and usually 4 or more, every year between 1977 and 2001. These have now all been measured with the SuperCOSMOS measuring machine (Hambly et al. 2001), and the scans and catalogues form part of the SuperCOSMOS Science Archive.

Although the SuperCOSMOS measures are superior in many ways to the earlier COSMOS measures, the SSA catalogues are also based on measures with a low detection threshold in order to maximize the depth of the survey. This again has the effect that the double quasar images are not resolved, and so we retrieved the original digitized mapping mode scans with a view to using more sophisticated photometric routines to measure the two images separately. Fig. 4 shows cut-outs of the double quasar images from two of the plates from the quasar variability survey. The exposures were taken in 1977 and 1986, and illustrate the change in magnitude difference between the two images over 9 years.

To measure the light curves we first extracted a square array from the SuperCOSMOS scan of each plate of side 8 arcmin and centred on Q2138-431. We then selected 18 stars in this field, spanning the magnitudes of the two quasar images, with which to construct a local photometric sequence. These stars were then identified in the  $g$ -band frame of the area from the DES survey. Taking advantage of the linearity of the CCD frames as opposed to the non-linear reciprocity failure of the photographic plates, we used the GAIA photometric package to measure the magnitudes of the sequence stars. The DES  $g$ -band and the photographic  $B_J$ -band are very similar, with an effective wavelength of  $4670 \text{ \AA}$ , and we could detect no significant colour term.

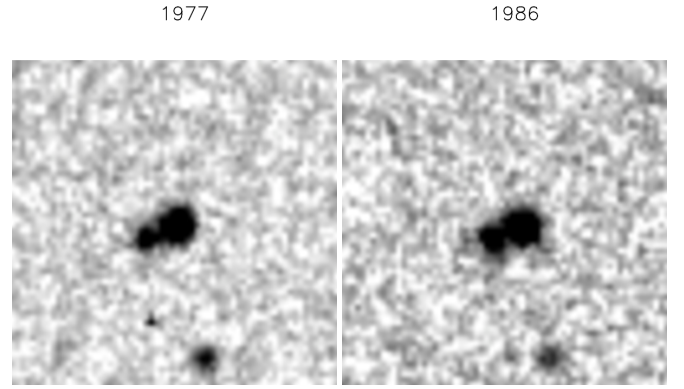


**Figure 4.** The two frames are from photographic plates taken by the UK 1.2m Schmidt telescope, and scanned by the SuperCOSMOS measuring machine at the Royal Observatory, Edinburgh. They illustrate the material on which the quasar light curves are based, and the change in magnitude difference between the two quasar images in the centre, over a period of 9 years. Image A to the right has decreased in brightness by about 0.5 magnitudes relative to image B on the left. Also included near the bottom of the plot is a standard star. The plots are approximately 40 arcsec on a side, and north is up the page, east to the left.

On this basis we used the  $g$ -band measures of the sequence stars to directly calibrate the  $B_J$  photographic images.

The first stage in the calibration was to transform the transmission values of the SuperCOSMOS scans to  $I$ , the intensity of light incident on the photographic plate, using the relation:

$$I \propto \left( \frac{T_c}{T} \right)^{1/\gamma} \quad (3)$$

where  $T$  is the transmission through exposed emulsion, and  $T_c$  through clear plate.  $\gamma$  is the gradient of the linear part of the response curve which in the first instance we set to 2.5. However,  $\gamma$  is basically a scaling factor which becomes redundant with the sequence star calibration.

The next step was to measure the magnitudes of the 18 sequence stars and two quasar images on each of the 79 plate scans from the SuperCOSMOS archive which were available for incorporation into the light curves. To do this, the transmission values were transformed to intensity using equation (3), and the resulting arrays converted to FITS files for analysis with the GAIA photometry package. Then for each plate the sequence star and quasar images were measured with the aperture photometry routine to give a quasi-linear relative flux, and thence converted to instrumental magnitudes. Using an aperture of radius 2 arcsec, the two quasar images were easily resolved on all plates. The final step was to transform these instrumental magnitudes to the sequence star magnitudes using a least squares third order polynomial fit. This transformation was then used to evaluate the true magnitudes of the two quasar images in the  $B_J$  passband.

The top panel of Fig. 5 shows the light curves for the two quasar images from 1977 to 2001. The error bars are derived from the dispersion about the calibration curve, and are typically about 0.05 magnitudes, with little dependence on brightness. The long term trend of the light curves is better seen in the middle panel of Fig. 5 where the observations for each year are averaged with a weighted mean. Little is lost by this procedure, as in most years the plates were taken within a period of about three months, and are not useful for measuring changes within the year. It will be seen that until 1985 the difference between the two light curves averaged around

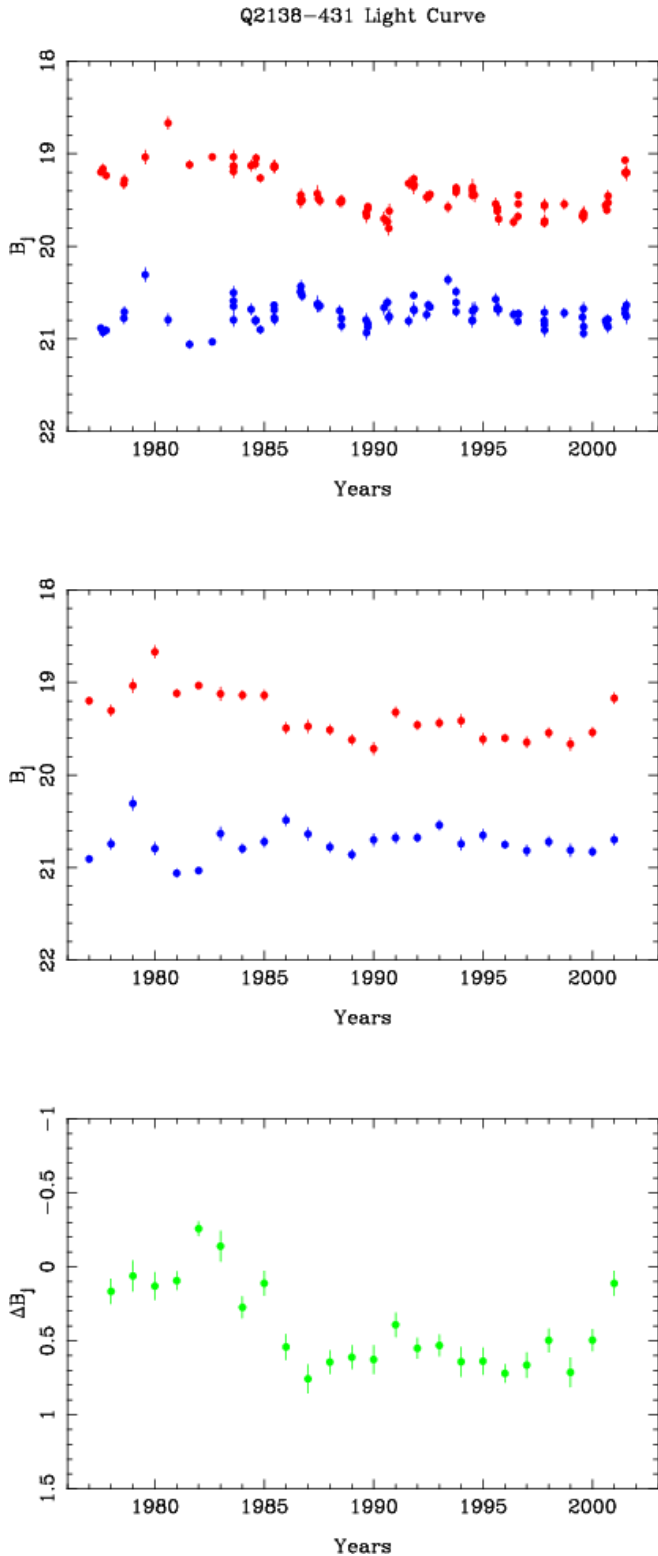


**Figure 5.** The top panel shows a 25 year light curve for image A (red) and image B (blue) of the double quasar Q2138-431, from SuperCOSMOS measures of a long series of UK 1.2m Schmidt plates in the  $B_J$  passband. The middle panel shows the same data, binned in yearly intervals. The bottom panel shows the difference light curve for the A and B images, with the observed lag of 1 year for image A removed.

**Table 2.** Correlation coefficients for time lags between images A and B of Q2138-431.

B leads A by (years)	2	1	0	-1	-2
1977 – 1985	+0.04	+0.70	+0.04	-0.69	-0.59
1986 – 1994	-0.20	+0.61	+0.31	+0.04	+0.18

1.5 magnitudes. After this image A dimmed, and the difference decreased by about 0.3 magnitudes. In the event that the double quasar is a gravitational lens system, we would expect intrinsic variations in the quasar to show up in both light curves, separated by a time interval corresponding to the difference in light travel time to the two quasar images. In addition, it is clear from large scale monitoring programmes of gravitational lenses that in most lensed systems the quasar images also vary independently of each other, which is generally accepted to be the result of microlensing by stellar mass bodies along the line of sight (Tewes et al. 2013). To look for a time lag between variations in the two images, and minimise the effects of microlensing, we split the light curves into two sections defined by the larger and smaller average magnitude differences, and measured the correlation coefficient for different time lags. The results are displayed in Table 2, and show for both time intervals a strong correlation between the two light curves when image B leads image A by one year. Given the poor time resolution of the light curves, this result should not be taken too seriously, but the existence of a time lag provides confirmation that Q2138-431 is a gravitational lens, and is a starting point for a more precise measurement.

The bottom panel of Fig. 5 shows the difference between the two light curves in the middle panel, with the curve for image B shifted back one year. The zero-point for the difference curve can be calculated from the magnitude difference of the two images in the infrared, where due to the size of the emitting region the effects of microlensing are negligible (Blackburne et al. 2011). From the  $J$ -band frames used for the detection of the lensing galaxy we find for the magnitude difference  $J_A - J_B = -1.77$ , which we use as the zero-point for the difference curve in the bottom panel of Fig. 5. This now shows the true differential effect of microlensing.

## 5 DISCUSSION

The idea behind this paper is to review the status of the double quasar Q2138-431 by taking advantage of improved observational data since its discovery in 1997. At the time the case for classifying it as a gravitational lens was very strong. The spectra were almost identical, as illustrated in Figures 1 and 2 of Hawkins et al. (1997), and for two randomly selected quasars this is very unlikely as illustrated in Figure 4 of Hawkins et al. (1997). There is of course the possibility that two quasars evolving in the same cluster environment could acquire the same observational characteristics, but the actual mechanism by which this could happen consistent with our knowledge of cluster evolution is far from clear. The one sticking point in the way of classifying the system as a gravitational lens was the failure to find a lensing galaxy.

Attempts to find a lensing galaxy by Hawkins et al. (1997) were mainly focussed on deep CCD observations in the  $R$ -band. They also reported observations in the  $K$ -band, but their frame is of a similar depth to the  $K_s$ -band frame in Fig. 2, and barely detects image B of

the quasar. Their  $R$ -band frame goes much deeper, and they derive a limit to the lensing galaxy brightness of  $R > 23.8$ . With this faint upper limit to the brightness and an estimate of the lens mass they derive a very large lower limit to the mass-to-light ratio of any lensing galaxy. Their lens mass is similar to the one we derive from mass modelling, but for reasons which are not clear Hawkins et al. (1997) appear to assume zero redshift luminosities, and do not take into account the very large  $K$  and evolutionary corrections associated with a distant galaxy. When these are allowed for, it seems unlikely that the galaxy we have detected in the  $J$ -band would have been detected by Hawkins et al. (1997) in their  $R$ -band frame for redshifts  $z \gtrsim 0.6$ .

Based on measurements of random fluctuations in the sky background, the object revealed after PSF subtraction in Fig. 3 is a  $5\sigma$  detection. Its appearance is similar to other faint galaxies in the surrounding 10 arcmin field, where the presence of an optical counterpart confirms their identity as galaxies. A good example is the faint galaxy to the south-east of the quasar system, used by Hawkins et al. (1997) to put limits on the  $R$ -band magnitude of a lensing galaxy. This galaxy is also clearly visible on deep  $r$ - and  $i$ -band frames from the DES survey, and is detected near the limit of the  $J$ -band frame in Fig. 3. There is in addition some indication of other faint galaxies in the vicinity of image A of the quasar. We have also searched the field for artefacts which might be mistaken for faint galaxies, but these are confined to single pixels, presumably cosmic ray tracks.

The value obtained for the mass-to-light ratio of the lens in Section 3 of  $M_{\odot}/L_{\odot} = 9.0$  assumes a redshift of  $z = 0.6$  based on non-detection of the lens in the  $i$ -band. As this redshift is essentially a lower limit, we investigated the effect of increasing it to  $z = 1.0$  and derived  $M_{\odot}/L_{\odot} = 8.2$  for the lensing galaxy. This small change in  $M_{\odot}/L_{\odot}$  is due to the fact that an increase in redshift results in larger values for both luminosity and mass which tend to cancel out in the mass-to-light ratio. Our value of  $M_{\odot}/L_{\odot}$  lies quite close to the relation between mass and mass-to-light found by Cappellari et al. (2006), and thus adds to a consistent picture of the double quasar as a gravitational lens.

The mass modelling of Q2138-431 turned out to be straightforward. This was not unexpected, as the lensing galaxy lies close to the line of centres of the quasar images, and roughly in the position one would expect given their brightness ratio. This contrasts strongly with for example the asymmetric Q0957+561 (Fadely et al. 2010), and more closely resembles HE1104-1805 (Sluse et al. 2012), another wide separation binary. This simplicity of modelling is important if Q2138-431 is to be used for measuring the Hubble constant, where the accuracy with which light travel time to the two images can be modelled is the most important factor limiting the accuracy of the result.

The software package of Keeton (2001) allows for the estimation of the time delay between two images of the modelled system, assuming a value for the Hubble constant. We applied this procedure to our model of Q2138-431 using a canonical value  $H_0 = 71 \text{ km s}^{-1} \text{ Mpc}^{-1}$  which implied a time lag with image B leading image A by 410 days. This is consistent with our crude estimate of 1 year from yearly observations, and hopefully can provide a starting point for a well sampled photometric monitoring programme designed to measure the value of  $H_0$ . For this calculation we assumed a lens redshift  $z = 0.6$ , equal to the lower limit derived in Section 3. Increasing the lens redshift results in a larger predicted time lag. For example a lens redshift of  $z = 1.0$  implies a time lag of 1130 days, which suggests that the true lens redshift is not much greater than our lower limit of  $z \gtrsim 0.6$ .

In the discovery paper of the double quasar Q2138-431 (Hawkins

et al. 1997), the strongest evidence supporting the gravitational lens hypothesis was the close similarity of the spectra of the two quasar images, and the very small difference between their redshifts. However, the authors concluded that without the detection of a lensing galaxy the claim that the system was a gravitational lens was insecure. In this paper we have brought together a number of new lines of argument to support the classification of Q2138-431 as a gravitational lens. The detection of the lensing galaxy is perhaps the most conclusive, but the simplicity of the mass model, the derivation of a plausible mass-to-light ratio, and the detection of a time lag between the light curves of the two quasar images in agreement with the mass model help to provide a consistent picture of a gravitational lens system. The measurement of the redshift of the lensing galaxy and the accurate determination of the time lag between the two images should then provide an excellent basis for a reliable estimate of the value of the Hubble constant.

## 6 CONCLUSIONS

In this paper we have re-examined the question of whether the double quasar Q2138-431 is a gravitational lens system. The system was discovered as part of a survey for quasars based on their variability, and elongated images were included as possible detections of gravitational lenses. Early analysis of Q2138-431 (Hawkins et al. 1997) showed it to comprise two quasar images separated by 4.5 arcsec, with almost identical spectra and redshifts. This provided strong evidence for a gravitational lens, but deep CCD photometry in the  $R$ -band failed to reveal a lensing galaxy. The authors thus concluded that there was insufficient evidence to definitively identify the system as a gravitational lens.

With the advent of more recent deep photometric surveys, especially in the infrared, we searched again for a lensing galaxy. In this case we successfully detected a candidate lens on a deep  $J$ -band frame from the VISTA Science Archive. The apparent magnitude of the  $5\sigma$  detection was measured to be  $J = 20.68$ , and non-detection in the optical bands implied a redshift  $z \gtrsim 0.6$ .

The wide separation of the quasar images at 4.481 arcsec and the apparent simplicity of the lens system make Q2138-431 an attractive candidate for the measurement of the Hubble constant, which would require mass modelling of the system. Based on our measurements of the positions of the quasar images and lensing galaxy we were able to obtain a satisfactory fit with a SIE +  $\gamma$  model, implying an estimated mass for the lens of  $m_{\text{lens}} = 1.31 \times 10^{12} M_{\odot}$ . Combining this with the infrared photometry in the  $J$ -band gives a mass-to-light ratio  $M_{\odot}/L_{\odot} = 9.0$  for the lensing galaxy.

The estimation of the Hubble constant in a gravitational lens system also requires a measurement of the time delay or difference in light travel time between the quasar images. We were able to make a preliminary assessment of this from an archival photographic monitoring programme covering 21 years. Although the effective time resolution of the survey was only about 1 year, we were able to show by cross-correlating the light curves of the two quasar images that image B leads image A by about a year. It was possible to estimate from our mass model that the expected time delay was about 410 days, consistent with the rough value from the light curve analysis.

The overall conclusion of this paper is that the double quasar Q2138-431 is confirmed as a gravitational lens system. The close similarity of the spectra, the detection of the lensing galaxy, the plausible mass-to-light ratio, and the measurement of a time delay between the two images in agreement with predictions from the mass model provide a consistent picture of a gravitational lens. Q2138-

431 appears to be a system well suited for the measurement of the Hubble constant. The wide separation of the quasar images should make measuring the time delay from photometry of the light curves straightforward, and the simplicity of the system should enable accurate modelling to estimate the value of the Hubble constant.

## ACKNOWLEDGEMENTS

I am most grateful to Nigel Hambly for retrieving the SuperCOSMOS scans used for constructing the light curves.

## DATA AVAILABILITY

The data upon which this paper is based are all publicly available and are referenced in Section 2, with some additional comments in the text.

## REFERENCES

- Abbott T.M.C. et al., 2018, *ApJS*, 239, 18  
 Blackburne J.A., Pooley D., Rappaport S., Schechter P.L., 2011, *ApJ*, 729, 34  
 Cappellari M. et al., 2006, *MNRAS*, 366, 1126  
 Choi J., Dotter A., Conroy C., Cantiello M., Paxton B., Johnson B.D., 2016, *ApJ*, 823, 102  
 D’Souza R., Vegetti S., Kauffmann G., 2015, *MNRAS*, 454, 4027  
 Eigenbrod A. et al., 2005, *A&A*, 436, 25  
 Fadely R., Keeton C.R., Nakajima R., Bernstein G.M., 2010, *ApJ*, 711, 246  
 Fohlmeister J. et al., 2008, *ApJ*, 676, 761  
 Hambly N.C., Irwin M.J., MacGillivray H.T., 2001, *MNRAS*, 326, 1295  
 Hawkins M.R.S., 1996, *MNRAS*, 415, 2744  
 Hawkins M.R.S., 1997, *A&A*, 328, L25  
 Hawkins M.R.S., 2020, *A&A*, 643, A10  
 Hawkins M.R.S., Clements D., Fried J.W., Heavens A.F., Véron P., Minty E.M., van der Werf P., 1997, *MNRAS*, 291, 811  
 Jordi K., Grebel E.K., Ammon K., 2006, *A&A*, 460, 339  
 Keeton C.R., 2001, arXiv:astro-ph/0102340  
 MacGillivray H.T., Stobie R.S., 1984, *Vistas Astron.*, 27, 433  
 Mannucci F. et al., 2001, *MNRAS*, 326, 745  
 McKean J.P. et al., 2005, *MNRAS*, 356, 1009  
 McKean J.P. et al., 2010, *MNRAS*, 404, 749  
 Oguri M. et al., 2008, *ApJ*, 676, L1  
 Poggianti B.M., 1997, *A&AS*, 122, 399  
 Popović L.Č. et al., 2010, *ApJ*, 721, L139  
 Sluse D., Chantry V., Magain P., Courbin F., Meylan G., 2012, *A&A*, 538, A99  
 Suyu S.H. et al., 2013, *ApJ*, 766, 70  
 Tewes M., Courbin F., Meylan G., 2013, *A&A*, 553, A120  
 Trujillo I., Aguerri J.A.L., Cepa J., Gutiérrez C.M., 2001, *MNRAS*, 328, 977  
 Walsh D., Carswell R.F., Weymann R.J., 1979, *Nature*, 279, 381  
 Wong K.C. et al., 2017, *MNRAS*, 465, 4895

This paper has been typeset from a  $\text{\TeX}/\text{\LaTeX}$  file prepared by the author.